Widespread mitochondrial depletion via mitophagy does not compromise necroptosis

Stephen W.G. Tait[1,^,*], **Andrew Oberst**[2,*], **Giovanni Quarato**[3,*], **Sandra Milasta**[3], **Martina Haller**[1], **Ruoning Wang**[4], **Maria Karvela**[1], **Gabriel Ichim**[1], **Nader Yatim**[3,5,6], **Matthew L. Albert**[5,6], **Grahame Kidd**[7], **Randall Wakefield**[8], **Sharon Frase**[8], **Stefan Krautwald**[9], **Andreas Linkermann**[9], and **Douglas R. Green**[3,^]

[1]CR-UK Beatson Institute, Institute of Cancer Sciences, University of Glasgow, Switchback Road, Glasgow, G61 1BD, U.K.

[2]Department of Immunology, University of Washington, 1959 NE Pacific St., Seattle, WA 98195, U.S.A.

[3]Department of Immunology, St. Jude Children's Research Hospital, 262 Danny Thomas Place, Memphis, TN 38105, U.S.A.

[4]Center for Childhood Cancer and Blood Disease, The Research Institute at Nationwide Children's Hospital Department of Pediatrics, Ohio State University School of Medicine 700 Children's Drive, Columbus, OH 43205, U.S.A.

[5]Unité d'Immunobiologie des Cellules Dendritiques, Department of Immunology, Institut Pasteur, 25 Rue du Docteur Roux, 75724, Paris, France.

[6]INSERM U818, Department of Immunology, Institut Pasteur, 25 Rue du Docteur Roux, 75724, Paris, France.

[7]Department of Neurosciences, Lerner Research Institute, Cleveland Clinic, Cleveland, Ohio 44195, U.S.A.

[8]Cell and Tissue Imaging Center, St. Jude Children's Research Hospital, 262 Danny Thomas Place, Memphis, TN 38105, U.S.A.

[9]Division of Nephrology and Hypertension, Christian-Albrechts-University, Kiel, Germany.

Summary

Programmed necrosis (or necroptosis) is a form of cell death triggered by the activation of receptor interacting protein kinase-3 (RIPK3). Several reports have implicated mitochondria and mitochondrial reactive oxygen species (ROS) generation as effectors of RIPK3-dependent cell

death. Here, we directly test this idea by employing a method for the specific removal of mitochondria via mitophagy. Mitochondria-deficient cells were resistant to the mitochondrial pathway of apoptosis, but efficiently died via TNF-induced, RIPK3-dependent programmed necrosis or as a result of direct oligomerization of RIPK3. Although the ROS scavenger butylated hydroxyanisol (BHA) delayed TNF-induced necroptosis, it had no effect on necroptosis induced by RIPK3 oligomerization. Further, while TNF-induced ROS production was dependent on mitochondria, the inhibition of TNF-induced necroptosis by BHA was observed in mitochondria-depleted cells. Our data indicate that mitochondrial ROS production accompanies, but does not cause, RIPK3-dependent necroptotic cell death.

Introduction

Apoptosis and programmed necrosis are two functionally linked cell death pathways that can be triggered by ligation of members of the "death receptor" (DR) family of cell surface receptors. Apoptosis is orchestrated by activation of the caspase family of cysteine proteases whereas programmed necrosis is initiated by the receptor interacting protein kinase (RIPK) family members RIPK1 and RIPK3. Signaling through DRs such as TNFR1 can lead to either apoptosis through activation of Caspase-8, or to programmed necrosis via RIPK1-RIPK3 signaling (He et al., 2009), and the latter is inhibited by the action of a heterodimer of Caspase-8 and the Caspase-8-like molecule, c-FLIP$_L$ (Dillon et al., 2012; Oberst et al., 2011). The signaling events connecting receptor ligation to RIPK3 activation have been extensively studied (Green et al., 2011). In contrast, the mechanisms by which RIP3 kinase activity leads to cell death are less clear, but several studies have implicated mitochondria as downstream effectors of the process (Vanden Berghe et al., 2010; Wang et al., 2012; Zhang et al., 2009). Several reports have also indicated a requirement for ROS production in the execution of RIPK3-dependent programmed necrosis (Cho et al., 2009; Kim et al., 2007; Lin et al., 2004; Vanden Berghe et al., 2010; Vanlangenakker et al., 2011; Zhang et al., 2009). We sought to directly test the roles for mitochondria and mitochondrial ROS in necroptosis.

Results

Necroptosis executes independently of mitochondrial permeability transition

During apoptosis (Goldstein et al., 2000; Marzo et al., 1998) and in some forms of necrosis (Baines et al., 2005) the mitochondrial transmembrane potential (ψm) dissipates prior to loss of plasma membrane integrity. We examined ψm during necroptosis, induced by treatment with tumor necrosis factor (TNF) plus benzyloxycarbonyl-Val-Ala-DL-Asp-fluoromethylketone (zVAD). We found that loss of ψm did not occur until after the plasma membrane became permeable (Figure 1A, Supplemental Movie 1) suggesting that necroptosis does not require mitochondrial permeability transition (MPT), which immediately dissipates ψm (Marzo et al., 1998). Supporting this, and in contrast to RIPK3 deletion, loss of cyclophilin D (a key component of the MPT pore (Baines et al., 2005)) failed to rescue embryonic lethality observed in Caspase-8 deficient mice (Figure 1B). These and other data (Ch'en et al., 2011) strongly suggest that if mitochondria act as important effectors of necroptosis, it is not through the MPT.

In order to definitively determine the importance of mitochondria as potential effectors in necroptosis, we sought to generate mitochondria-deficient cells. Previous studies have shown that Parkin induces removal of mitochondria lacking Ψm through the process of mitophagy, and that extensive Parkin-mediated mitophagy can fully deplete all mitochondria in a cell (Narendra et al., 2008). We therefore generated SVEC or 3T3-SA cells stably expressing YFP-Parkin and treated them with the protonophore carbonylcyanide *m*-chlorophenylhydrazone (CCCP) for 2 days. Mitochondrial content was assessed by immunostaining for the mitochondrial protein Tom20 (Figure 1C) or by Western blotting for the mitochondrial proteins Tom20 and cytochrome *c* (Figure 1D and S1A). Quantitative single-cell analysis demonstrated that at least 80% of Parkin-expressing, CCCP-treated SVEC or 3T3-SA cells were depleted of mitochondria as evidenced by loss of punctate, mitochondrial Tom20 staining (Figure 1C). Time-course analysis of mitochondrial depletion revealed initial mitochondrial fragmentation followed by aggregation and progressive depletion to below the level of detection (Figure S1B), as in previous studies (Lee et al., 2010; Narendra et al., 2010). Consistent with a penetrant removal of mitochondria, short-term treatment with CCCP completely abolished the clonogenic capacity of Parkin-expressing SVEC and 3T3-SA cells (Figure S1C). We further observed a dramatic loss of mitochondrial cytochrome *c* and Tom20 protein in SVEC Parkin- or 3T3-SA Parkin-expressing cells following CCCP treatment (Figure 1D and S1A). Treated cells were selectively depleted of mitochondrial DNA (Figure 1E), lacked oxygen consumption (Figure 1F), and were defective in glutaminolysis (Figure S1D). Mitochondria-deficient cells were viable and persisted in culture for up to several days (Figure S1E), as previously described (Narendra et al., 2008).

TNF dependent necroptosis does not require mitochondria

To rigorously determine the extent of mitochondrial depletion, we carried out transmission electron microscopy (TEM) and 3D electron microscopy (3D-EM) of Parkin-expressing 3T3-SA cells. CCCP treatment of these cells effectively eliminated mitochondria to undetectable levels (Figures 2A, B and C, Supplemental Movies 2 and 3). It should be noted that while mitochondria were nearly completely depleted, as assessed by 3D-EM, a low level of mitochondrial DNA was nevertheless detected (Figure 1E), which may represent un-degraded DNA in lysosomes. These cells were subjected to treatment for the induction of necroptosis, using TNF plus zVAD, with or without the RIPK1 inhibitor, necrostatin-1 (Nec1) for 8 hours. Despite nearly complete depletion of mitochondria, these cells displayed extensive Nec-1-inhibitable cell death in response to this treatment, as detected by uptake of propidium iodide (PI, 20% vs 21% in control cells without CCCP treatment, data not shown).

3T3-SA or SVEC cells expressing Parkin then were treated with CCCP for 2 days, followed by treatment with TNF plus zVAD to induce necroptosis, with or without Nec-1. Alternatively, cells were treated with TNF plus cycloheximide (CHX), staurosporine (STS) or actinomycin D (ActD) to trigger apoptosis. Cell death was measured by PI exclusion. Immunoblotting for cytochrome *c* and Tom20 demonstrated effective removal of mitochondria in Parkin-expressing 3T3-SA or SVEC cells following CCCP treatment (Figure 1D and S1A). Mitochondria-depleted 3T3-SA and SVEC cells expressing Parkin

displayed resistance to apoptosis (Figure 2D). Importantly, TNF plus zVAD-induced necroptosis occurred to the same extent in both 3T3-SA and SVEC Parkin-expressing cells irrespective of CCCP treatment, and this was inhibited by Nec-1 (Figure 2D). Cell death induced in 3T3-SA cells by TNF plus zVAD (necroptosis) or Act D (apoptosis) was then examined by live cell imaging. Although mitochondria-depleted CCCP-treated 3T3-SA cells expressing Parkin were protected from Act D-induced apoptosis (Figure 2E), the kinetics and extent of necroptosis were identical in 3T3-SA cells expressing Parkin irrespective of CCCP treatment (Figure 2F). Collectively these data demonstrate that mitochondria are not required for TNF plus zVAD-induced necroptosis.

Direct induction of programmed cell death demonstrates a role for mitochondria in apoptosis, but not in programmed necrosis

To gain a better understanding of the effector mechanisms acting downstream of RIPK3 in programmed necrosis, we constructed a system in which this form of cell death is specifically induced independently of the pleiotropic effects of TNF. We employed inducible dimerization, which uses modified regions of the protein FKBP12 and a rapamycin-derived dimerizer. We generated an induced-active (ac) form of RIPK3 by fusing tandem dimerization domains to the RIPK3 C-terminus (Figure 3A). Similarly, an acCaspase-8 was utilized to trigger apoptosis, as described previously (Muzio et al., 1998; Oberst et al., 2010).

To characterize the function of acRIPK3, we stably expressed either full-length murine RIPK3 or acRIPK3 in NIH-3T3 cells, which do not express endogenous RIPK3 (He, et al., 2009). The levels of expression of acRIPK3 in these cells and endogenous RIPK3 in 3T3-SA cells appeared similar (Figure S2A). When treated with TNF plus zVAD, we found that 3T3 NIH cells expressing either RIPK3 or acRIPK3 underwent cell death, and that this death was inhibited by the RIPK1 inhibitor Nec-1 (Figure 3B). However, when treated with dimerizer, we found that acRIPK3-expressing cells underwent rapid cell death, while RIPK3-expressing cells were unaffected. The cell death observed upon dimerizer-induced activation of acRIPK3 did not require zVAD addition, and was not inhibited by Nec-1, consistent with direct activation of RIPK3 by dimerization (Figure 3B).

Mixed lineage kinase like (MLKL) is an essential mediator of RIPK3-dependent necrosis (Sun et al., 2012; Wu et al., 2013; Zhao et al., 2012). Consistent with this role, knockdown of MLKL attenuated TNF plus zVAD-induced death of RIPK3-expressing 3T3 NIH cells, and cell death induced by either TNF plus zVAD or dimerizer treatment in 3T3 NIH cells expressing acRIPK3 (Figure S2B). AcRIPK3 oligomerization required the kinase activity of RIPK3 to cause necroptosis (Figure S2C), as expected (He, et al., 2009). Therefore, RIPK3 oligomerization most likely induces cell death by the same effector mechanism induced by TNF plus zVAD.

We next evaluated the effects of depleting mitochondria in cells expressing acCaspase-8 or acRIPK3. Parkin effectively depleted mitochondria in acCaspase-8 or acRIPK3 expressing NIH 3T3 cells (Figure S2D and E). We found that upon removal of mitochondria, cell death triggered by either TNF plus zVAD or dimerizer was unchanged with respect to extent (Figure 3C) or kinetics (Figure 3D). In contrast, in NIH-3T3 cells stably expressing

acCaspase-8, we found that depletion of mitochondria substantially blocked apoptosis induced dimerizer or ActD treatment (Figure 3E). The requirement for mitochondria in the Caspase-8-induced apoptotic response is consistent with the "type II" response to death receptor ligation, in which mitochondrial outer membrane permeabilization is required for antagonism of XIAP (Jost et al., 2009).

Roles for the mitochondrial phosphatase PGAM5 and the regulator of mitochondrial fission DRP1 in the execution of necroptosis were recently proposed (Wang et al., 2012). In line with its mitochondrial localization, PGAM5 was effectively depleted from Parkin expressing cells following CCCP treatment, whereas Drp-1 was unaffected (Figure S2F). However, we failed to observe a role for either protein in our systems (Figure S2). Knockdown of PGAM5, while depleting protein levels (Figure S2G) did not affect necroptosis induced by TNF or direct activation of acRIPK3 in NIH-3T3 cells (Figure S2H), nor in response to TNF plus zVAD treatment of 3T3-SA or SVEC cells expressing endogenous RIPK3 (Figure S2J). Although knockdown of DRP1 (Figure S2G) caused extensive mitochondrial fusion as expected (Figure S2I), we observed no effect on necroptosis (Figure S2H,J). While silencing of these proteins cannot be taken as a formal demonstration that they are not involved in necroptosis, our findings prohibited us from further exploring any possible extra-mitochondrial roles for PGAM5 or DRP1 in the process.

Elimination of mitochondria prevents necroptosis-associated ROS production, but does not alter RIPK3-dependent cell death

A role for mitochondria in necroptosis has been proposed, in large part, by its association with a ROS burst and the finding that the ROS scavenger, butylated hydroxyanisole (BHA) effectively delays cell death induced by TNF plus zVAD (He et al., 2011; Vanden Berghe et al., 2010). We found that TNF plus zVAD induced RIPK3-dependent ROS that was efficiently inhibited by BHA or by another scavenger, N-acetylcysteine (NAC) (Figure 4A). Strikingly, depletion of mitochondria prevented this ROS burst (Figure 4A). Similar results were found in 3T3-SA cells expressing Parkin (Figure S3B). However, while BHA effectively inhibited necroptosis induced by TNF plus zVAD, neither NAC nor mitochondrial depletion influenced cell death (Figure 4B and Figure S3A). This effect of BHA was not observed when necrosis was induced by direct activation of acRIPK3 (Figure 4C). Remarkably, the ability of BHA to partially inhibit necroptosis induced by TNF plus zVAD was also observed in cells that were depleted of mitochondria (Figure 4D).

The effect of BHA on necroptosis is therefore independent of mitochondrial ROS, and thus, an "off-target" effect. BHA has been shown to compromise a number of mitochondrial functions in addition to ROS production, including inhibition of Phospholipase-A2 (Festjens et al., 2006) which has also been implicated in necroptosis (Cauwels et al., 2003). However, the failure of BHA to influence necroptosis induced by oligomerization of acRIPK3, and our failure to identify a role for mitochondria in cell death induced by TNF plus zVAD or direct activation of RIPK3 suggest that any effects of BHA or other manipulations of mitochondrial functions (Wang et al., 2012) on necroptosis may act upstream of the engagement of RIPK3 activation.

Discussion

Our results strongly argue against a major role for mitochondria as effectors of necroptosis. These findings, as well as the striking rapidity with which RIPK3 activation leads to necrotic death (e.g., Figure S2C) suggests that the effect is unlikely to be via subtle metabolic processes (Zhang et al., 2009) or ROS (Cho et al., 2009). Nevertheless, as roles for necroptosis have been identified in developmental defects (Dillon et al., 2012; Oberst et al., 2011), ischemic injury (Linkermann et al., 2012), (Rosenbaum et al., 2010), and other pathologies (He et al., 2009), understanding the way in which RIPK3 mediates its lethal activity remains of great interest.

During the early exploration of the mechanisms of apoptosis, it was widely held that the process relied on nuclear events and/or mitochondrial ROS. Important progress was made when it was demonstrated that apoptotic cell death proceeds in cells from which nuclei had been removed (Jacobson et al., 1994; Schulze-Osthoff et al., 1994) and in cells from which mitochondrial DNA had been depleted (Jacobson et al., 1993). In our studies we followed a similar logic: if necroptosis is effected by mitochondria, then artificial depletion of mitochondria from a cell should impact the process of necroptosis. While our studies do not provide a final effector mechanism for this form of cell death, we conclude that efforts to link RIP kinase activation and MLKL to the mitochondria will not be informative in the elucidation of how cells die by this important process.

Experimental Procedures

Plasmids and retroviral transduction

mCherry-Parkin-IRES-zeocin and YFP-Parkin-IRES-zeocin were generated by ligating mCherry C1 Parkin and eYFP C1 Parkin (both provided by Dr. Richard Youle) into the LZRS vector (Tait et al., 2010) using standard cloning techniques (see also Supplemental Experimental Procedures).

Microscopy

Live-cell imaging was carried out using spinning disk confocal microscopy making use of a Marianas SDC imaging system (for Annexin V/PI/TMRE) or laser scanning microscopy using a Nikon A1R system (for Mitotracker Green) (see also Supplemental Experimental Procedures).

RNA interference and Western blot

Cells (5×10^4) were transfected with control or Smartpool RNAi duplexes (Dharmacon) targeting murine MLKL, PGAM5 or Drp-1. Duplexes were transfected twice on consecutive days with Lipofectamine 2000 (Invitrogen) according to the manufacturer's instructions. Cells were analysed 3 days following the initial transfection (see also Supplemental Experimental Procedures).

Clonogenicity assay, Treatments and Cell Death Assays

Cells were seeded in 12-well plates (5×10^3 cells per well) and treated +/− CCCP (12.5μM) two times over a 24-hour period after which it was washed out and replaced with complete media. Colonies were stained with methylene blue solution (1% w/v methylene blue in a 50:50 methanol/water solution) (see also Supplemental Experimental Procedures).

Seahorse Oxygen Consumption Assay, Mitochondrial DNA and ROS quantification

Respiration was measured using a Seahorse XF24 analyzer. Cells were seeded in plates coated with poly-L-lysine. After 5 hrs, the cells were loaded into the machine to determine the oxygen consumption rate (OCR) (see also Supplemental Experimental Procedures).

Generation of cyclophilinD-ko/caspase-8 het mice and statistical analysis

To generate cyclophilinD-ko/caspase-8 het mice, we crossed cyclophilin D-KO (B6;129-Ppif tm1Jmol/J, The Jackson Laboratory, Bar Harbor, Maine USA, Order No. 009071) mice that were previously published (Nakayama et al., 2007) with caspase-8/RIPK3-dko mice (Oberst et al., 2011) (see also Supplemental Experimental Procedures).

Supplementary Material

Refer to Web version on PubMed Central for supplementary material.

Acknowledgments

References

Baines CP, Kaiser RA, Purcell NH, Blair NS, Osinska H, Hambleton MA, Brunskill EW, Sayen MR, Gottlieb RA, Dorn GW, et al. Loss of cyclophilin D reveals a critical role for mitochondrial permeability transition in cell death. Nature. 2005; 434:658–662. [PubMed: 15800627]

Cauwels A, Janssen B, Waeytens A, Cuvelier C, Brouckaert P. Caspase inhibition causes hyperacute tumor necrosis factor-induced shock via oxidative stress and phospholipase A2. Nat Immunol. 2003; 4:387–393. [PubMed: 12652297]

Ch'en IL, Tsau JS, Molkentin JD, Komatsu M, Hedrick SM. Mechanisms of necroptosis in T cells. The Journal of experimental medicine. 2011; 208:633–641. [PubMed: 21402742]

Cho YS, Challa S, Moquin D, Genga R, Ray TD, Guildford M, Chan FK. Phosphorylation-driven assembly of the RIP1-RIP3 complex regulates programmed necrosis and virus-induced inflammation. Cell. 2009; 137:1112–1123. [PubMed: 19524513]

Dillon CP, Oberst A, Weinlich R, Janke LJ, Kang TB, Ben-Moshe T, Mak TW, Wallach D, Green DR. Survival function of the FADD-CASPASE-8-cFLIP(L) complex. Cell reports. 2012; 1:401–407. [PubMed: 22675671]

Festjens N, Kalai M, Smet J, Meeus A, Van Coster R, Saelens X, Vandenabeele P. Butylated hydroxyanisole is more than a reactive oxygen species scavenger. Cell Death Differ. 2006; 13:166–169. [PubMed: 16138110]

Goldstein JC, Waterhouse NJ, Juin P, Evan GI, Green DR. The coordinate release of cytochrome c during apoptosis is rapid, complete and kinetically invariant. Nature cell biology. 2000; 2:156–162.

Green DR, Oberst A, Dillon CP, Weinlich R, Salvesen GS. RIPKdependent necrosis and its regulation by caspases: a mystery in five acts. Molecular cell. 2011; 44:9–16. [PubMed: 21981915]

He S, Liang Y, Shao F, Wang X. Toll-like receptors activate programmed necrosis in macrophages through a receptor-interacting kinase-3-mediated pathway. Proc Natl Acad Sci U S A. 2011; 108:20054–20059. [PubMed: 22123964]

He S, Wang L, Miao L, Wang T, Du F, Zhao L, Wang X. Receptor interacting protein kinase-3 determines cellular necrotic response to TNF-alpha. Cell. 2009; 137:1100–1111. [PubMed: 19524512]

Jacobson MD, Burne JF, King MP, Miyashita T, Reed JC, Raff MC. Bcl-2 blocks apoptosis in cells lacking mitochondrial DNA. Nature. 1993; 361:365–369. [PubMed: 8381212]

Jacobson MD, Burne JF, Raff MC. Programmed cell death and Bcl-2 protection in the absence of a nucleus. EMBO J. 1994; 13:1899–1910. [PubMed: 8168488]

Jost PJ, Grabow S, Gray D, McKenzie MD, Nachbur U, Huang DC, Bouillet P, Thomas HE, Borner C, Silke J, et al. XIAP discriminates between type I and type II FAS-induced apoptosis. Nature. 2009; 460:1035–1039. [PubMed: 19626005]

Kim YS, Morgan MJ, Choksi S, Liu ZG. TNF-induced activation of the Nox1 NADPH oxidase and its role in the induction of necrotic cell death. Molecular cell. 2007; 26:675–687. [PubMed: 17560373]

Lee JY, Nagano Y, Taylor JP, Lim KL, Yao TP. Disease-causing mutations in parkin impair mitochondrial ubiquitination, aggregation, and HDAC6-dependent mitophagy. J Cell Biol. 2010; 189:671–679. [PubMed: 20457763]

Lin Y, Choksi S, Shen HM, Yang QF, Hur GM, Kim YS, Tran JH, Nedospasov SA, Liu ZG. Tumor necrosis factor-induced nonapoptotic cell death requires receptor-interacting protein-mediated cellular reactive oxygen species accumulation. The Journal of biological chemistry. 2004; 279:10822–10828. [PubMed: 14701813]

Linkermann A, Brasen JH, Himmerkus N, Liu S, Huber TB, Kunzendorf U, Krautwald S. Rip1 (receptor-interacting protein kinase 1) mediates necroptosis and contributes to renal ischemia/ reperfusion injury. Kidney Int. 2012; 81:751–761. [PubMed: 22237751]

Marzo I, Brenner C, Zamzami N, Susin SA, Beutner G, Brdiczka D, Remy R, Xie ZH, Reed JC, Kroemer G. The permeability transition pore complex: a target for apoptosis regulation by caspases and bcl-2-related proteins. J Exp Med. 1998; 187:1261–1271. [PubMed: 9547337]

Muzio M, Stockwell BR, Stennicke HR, Salvesen GS, Dixit VM. An induced proximity model for caspase-8 activation. The Journal of biological chemistry. 1998; 273:2926–2930. [PubMed: 9446604]

Nakayama H, Chen X, Baines CP, Klevitsky R, Zhang X, Zhang H, Jaleel N, Chua BH, Hewett TE, Robbins J, et al. Ca2+- and mitochondrial-dependent cardiomyocyte necrosis as a primary mediator of heart failure. J Clin Invest. 2007; 117:2431–2444. [PubMed: 17694179]

Narendra D, Kane LA, Hauser DN, Fearnley IM, Youle RJ. p62/SQSTM1 is required for Parkin-induced mitochondrial clustering but not mitophagy; VDAC1 is dispensable for both. Autophagy. 2010; 6:1090–1106. [PubMed: 20890124]

Narendra D, Tanaka A, Suen DF, Youle RJ. Parkin is recruited selectively to impaired mitochondria and promotes their autophagy. J Cell Biol. 2008; 183:795–803. [PubMed: 19029340]

Oberst A, Dillon CP, Weinlich R, McCormick LL, Fitzgerald P, Pop C, Hakem R, Salvesen GS, Green DR. Catalytic activity of the caspase-8-FLIP(L) complex inhibits RIPK3-dependent necrosis. Nature. 2011; 471:363–367. [PubMed: 21368763]

Oberst A, Pop C, Tremblay AG, Blais V, Denault JB, Salvesen GS, Green DR. Inducible dimerization and inducible cleavage reveal a requirement for both processes in caspase-8 activation. The Journal of biological chemistry. 2010; 285:16632–16642. [PubMed: 20308068]

Rosenbaum DM, Degterev A, David J, Rosenbaum PS, Roth S, Grotta JC, Cuny GD, Yuan J, Savitz SI. Necroptosis, a novel form of caspase-independent cell death, contributes to neuronal damage in a retinal ischemia-reperfusion injury model. J Neurosci Res. 2010; 88:1569–1576. [PubMed: 20025059]

Schulze-Osthoff K, Walczak H, Droge W, Krammer PH. Cell nucleus and DNA fragmentation are not required for apoptosis. J Cell Biol. 1994; 127:15–20. [PubMed: 7523418]

Sun L, Wang H, Wang Z, He S, Chen S, Liao D, Wang L, Yan J, Liu W, Lei X, et al. Mixed lineage kinase domain-like protein mediates necrosis signaling downstream of RIP3 kinase. Cell. 2012; 148:213–227. [PubMed: 22265413]

Tait SW, Parsons MJ, Llambi F, Bouchier-Hayes L, Connell S, Munoz-Pinedo C, Green DR. Resistance to caspase-independent cell death requires persistence of intact mitochondria. Dev Cell. 2010; 18:802–813. [PubMed: 20493813]

Vanden Berghe T, Vanlangenakker N, Parthoens E, Deckers W, Devos M, Festjens N, Guerin CJ, Brunk UT, Declercq W, Vandenabeele P. Necroptosis, necrosis and secondary necrosis converge on similar cellular disintegration features. Cell Death Differ. 2010; 17:922–930. [PubMed: 20010783]

Vanlangenakker N, Vanden Berghe T, Bogaert P, Laukens B, Zobel K, Deshayes K, Vucic D, Fulda S, Vandenabeele P, Bertrand MJ. cIAP1 and TAK1 protect cells from TNF-induced necrosis by preventing RIP1/RIP3-dependent reactive oxygen species production. Cell Death Differ. 2011; 18:656–665. [PubMed: 21052097]

Wang Z, Jiang H, Chen S, Du F, Wang X. The mitochondrial phosphatase PGAM5 functions at the convergence point of multiple necrotic death pathways. Cell. 2012; 148:228–243. [PubMed: 22265414]

Wu J, Huang Z, Ren J, Zhang Z, He P, Li Y, Ma J, Chen W, Zhang Y, Zhou X, et al. Mlkl knockout mice demonstrate the indispensable role of Mlkl in necroptosis. Cell Res. 2013; 23:994–1006. [PubMed: 23835476]

Zhang DW, Shao J, Lin J, Zhang N, Lu BJ, Lin SC, Dong MQ, Han J. RIP3, an energy metabolism regulator that switches TNF-induced cell death from apoptosis to necrosis. Science. 2009; 325:332–336. [PubMed: 19498109]

Zhao J, Jitkaew S, Cai Z, Choksi S, Li Q, Luo J, Liu ZG. Mixed lineage kinase domain-like is a key receptor interacting protein 3 downstream component of TNF-induced necrosis. Proc Natl Acad Sci U S A. 2012; 109:5322–5327. [PubMed: 22421439]

- Parkin-induced mitochondrial depletion can be used to define mitochondrial functions

- Mitochondrial depletion prevents TNF-induced ROS but not necroptosis

- Activated RIPK3-induced necroptosis proceeds normally in mitochondria-depleted cells

- The ROS scavenger, BHA, delays TNF-induced necroptosis in mitochondria-depleted cells
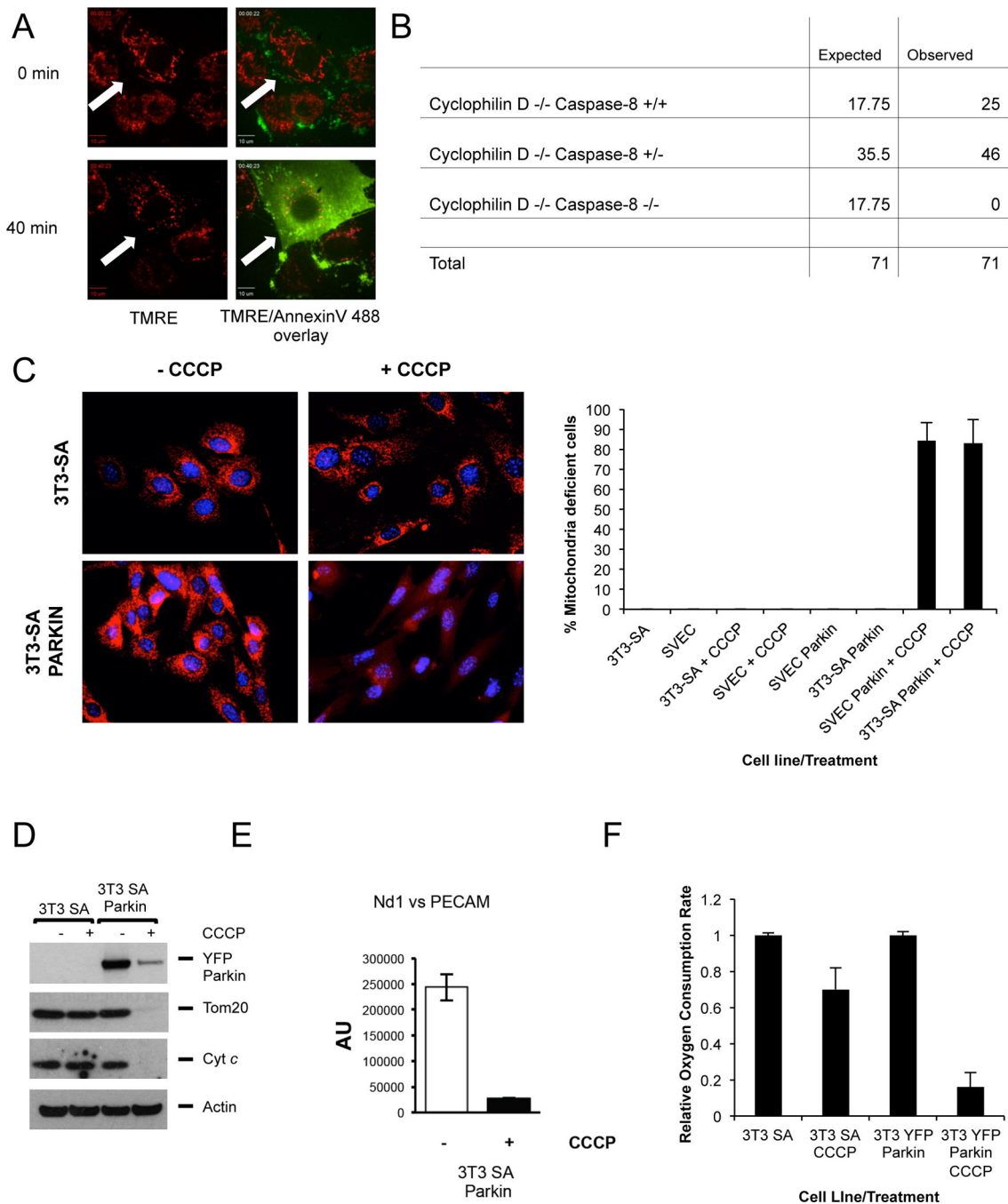
Figure 1. Necroptosis executes independently of mitochondrial permeability transition
A. SVEC cells were incubated with TMRE/Annexin V Alexa Fluor 488, treated with TNF+zVAD and imaged by live-cell confocal microscopy. Images following initial treatment and at the point of cell lysis are shown. Arrow denotes the same cell at different time-points **B.** Expected and observed frequency of caspase-8/cyclophilin D status in offspring from crosses of cyclophilin D −/− caspase 8 +/− mice. **C.** Left: Representative images of control or Parkin expressing 3T3-SA cells treated +/− CCCP for 48 hours and immunostained with anti-Tom20 antibody. Right: Quantitation of control or Parkin expressing 3T3-SA or SVEC cells treated +/− CCCP for 48 hours that lack mitochondrial Tom20 staining. A minimum of 100 cells were counted per condition per experiment. Error bars represent the standard deviation (S.D.) from the mean of 3 independent experiments. **D.**

Control or Parkin expressing 3T3-SA or cells were treated with CCCP for 48 hours and protein expression was monitored by Western blot. Actin was used as a loading control. **E.** Parkin expressing 3T3-SA cells were treated with CCCP for 48 hours and assayed for mtDNA copy number per nuclear genome. Error bars represent S.D. from the mean of triplicate samples. Data are representative of 3 independent experiments. The same pool of cells was used for the EM analysis in fig, 2A-B. **F.** Control or Parkin expressing 3T3-SA cells were treated with CCCP for 48 hours and oxygen consumption was determined and is displayed relative to the untreated control. Error bars represent S.D. from the mean of triplicate samples. Data are representative of 3 independent experiments. See also Figure S1 and Movie S1.
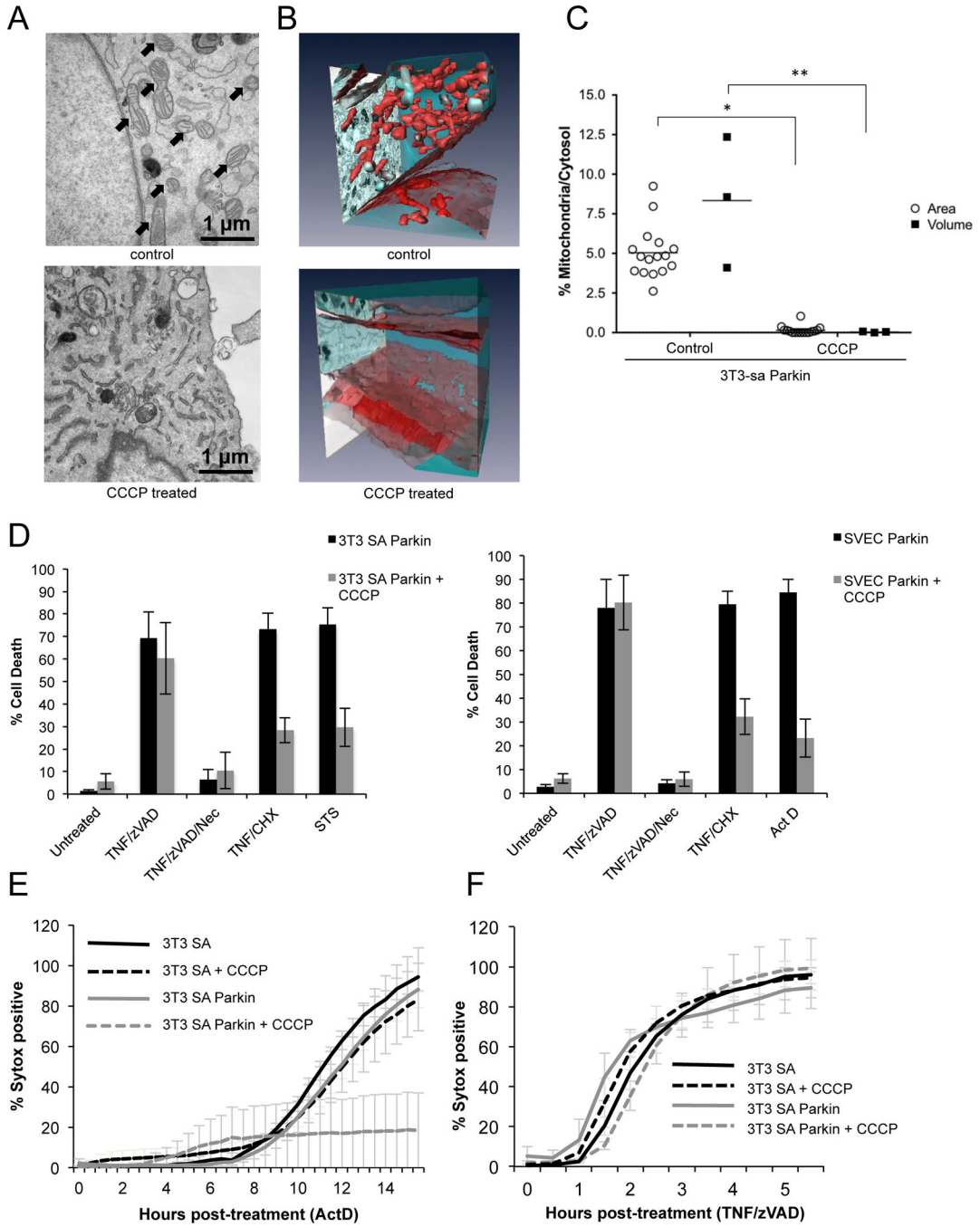
Figure 2. TNF dependent necroptosis does not require mitochondria

A. Representative TEM images of control or CCCP treated 3T3-SA Parkin expressing cells, arrows denote mitochondria. **B** Representative 3D-EM images of control or CCCP treated 3T3-SA Parkin expressing cells. Mitochondria are colored red and cytosol is colored blue. **B.** 3D-EM quantification of mitochondrial mass of Parkin expressing 3T3-SA treated with CCCP for 48 hours. Black squares represent the ratio of "Area Mitochondria/Area Cytosol" and expressed as percentages (%Area Mitochondria/Area Cytosol); white circles represent the percentage of the ratio "Volume Mitochondria/Volume Cytosol". For further information see *Materials and Methods*. *, P<0.0001, **, P<0.05. **C.** Control or Parkin expressing 3T3-SA or SVEC cells were treated with CCCP for 48 hours then treated with the indicated stimuli for 8 hours (TNF/zVAD, TNF/CHX) or

overnight with staurosporine (STS) or actinomycin D (ActD). Cell death was determined by propidium iodide (PI) positivity and flow cytometry. **D.** Mitochondria depletion was triggered in 3T3-SA cells by CCCP treatment for 48 hours, and cells were treated with ActD as indicated. Cell death was assayed using Sytox Green uptake over time in an IncuCyte imager. **E.** Mitochondria depletion was triggered in 3T3-SA cells by CCCP treatment for 48 hours, and cells were treated with TNF/zVAD as indicated. Cell death was assayed using Sytox Green uptake over time in an IncuCyte imager. Sytox positive cell counts were normalized to total cell numbers using the cell-permeable dye Syto24. Error bars represent the S.D. from the mean of 3 independent experiments. See also Movies S2 and S3.
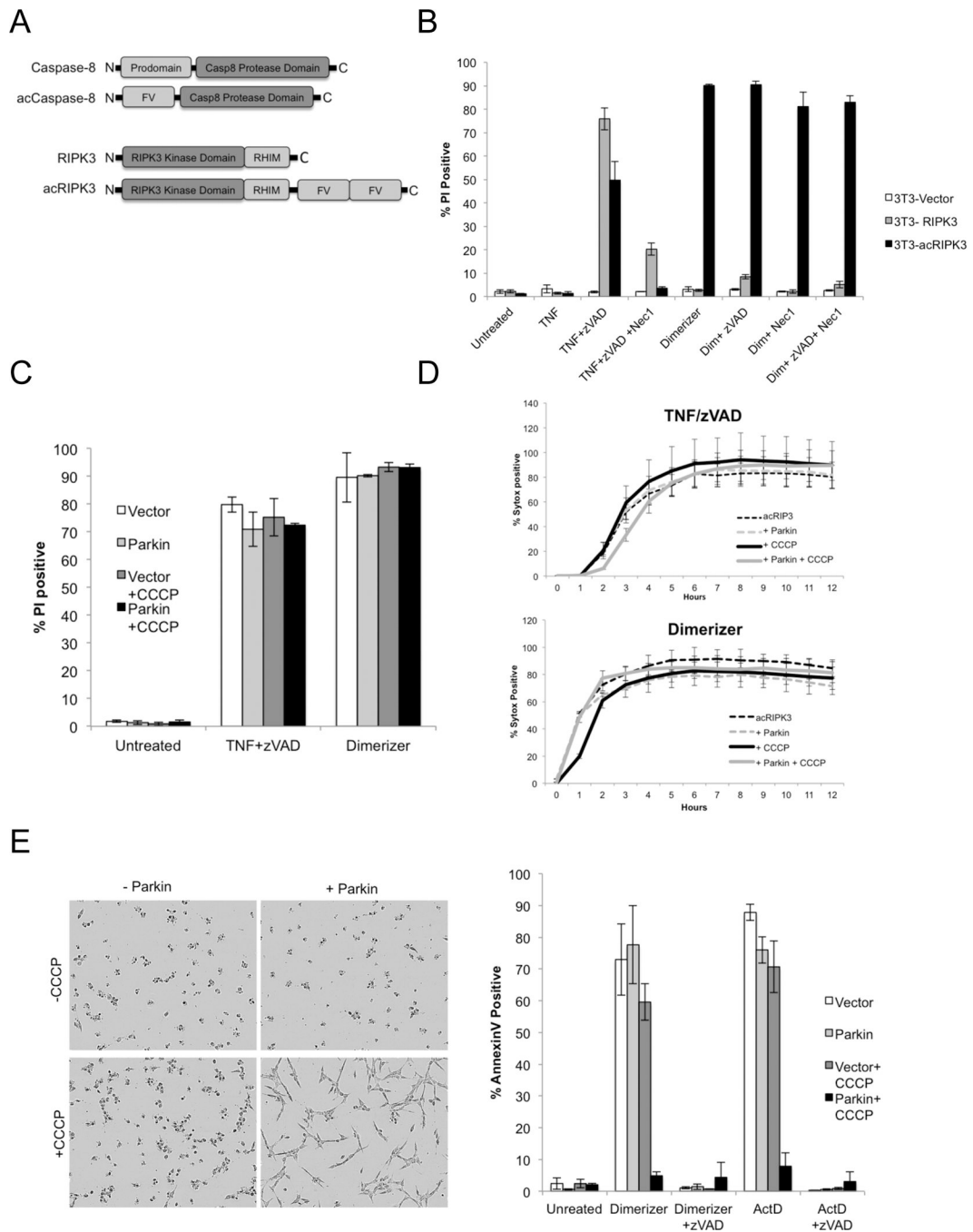
Figure 3. Direct induction of programmed cell death demonstrates a role for mitochondria in apoptosis, but not in programmed necrosis

A. Schematic representation of fusion proteins used to directly induce apoptosis (acCaspase-8) or programmed necrosis (acRIPK3) **B.** NIH-3T3 cells stably transduced with RIPK3 or acRIPK3 were treated as indicated, and cell death was determined by PI positivity and flow cytometry 4 hours later. **C**. NIH-3T3 cells expressing acRIPK3 as well as either LZRS vector or Parkin-LZRS were treated with CCCP as indicated to induce elimination of mitochondria. 48 hours later, cell death was induced using the treatments indicated. **D**. NIH-3T3 cells expressing acRIPK3 were treated to deplete mitochondria and cell death was quantified using an IncuCyte imager. Sytox positive cell counts were normalized to total cell numbers using the cell-permeable

dye Syto24. **E**. NIH-3T3 cells expressing acCaspase-8 as well as either LZRS vector or Parkin-LZRS were treated with CCCP as indicated to induce elimination of mitochondria as described in Figure 1. 48 hours later, cell death was induced using the treatments indicated, representative images (left) and percentage of cells displaying Annexin V positivity (right) was analyzed 8 hours after treatment by flow-cytometry. Error bars represent the S.D. from 3 replicate experiments. See also Figure S2.
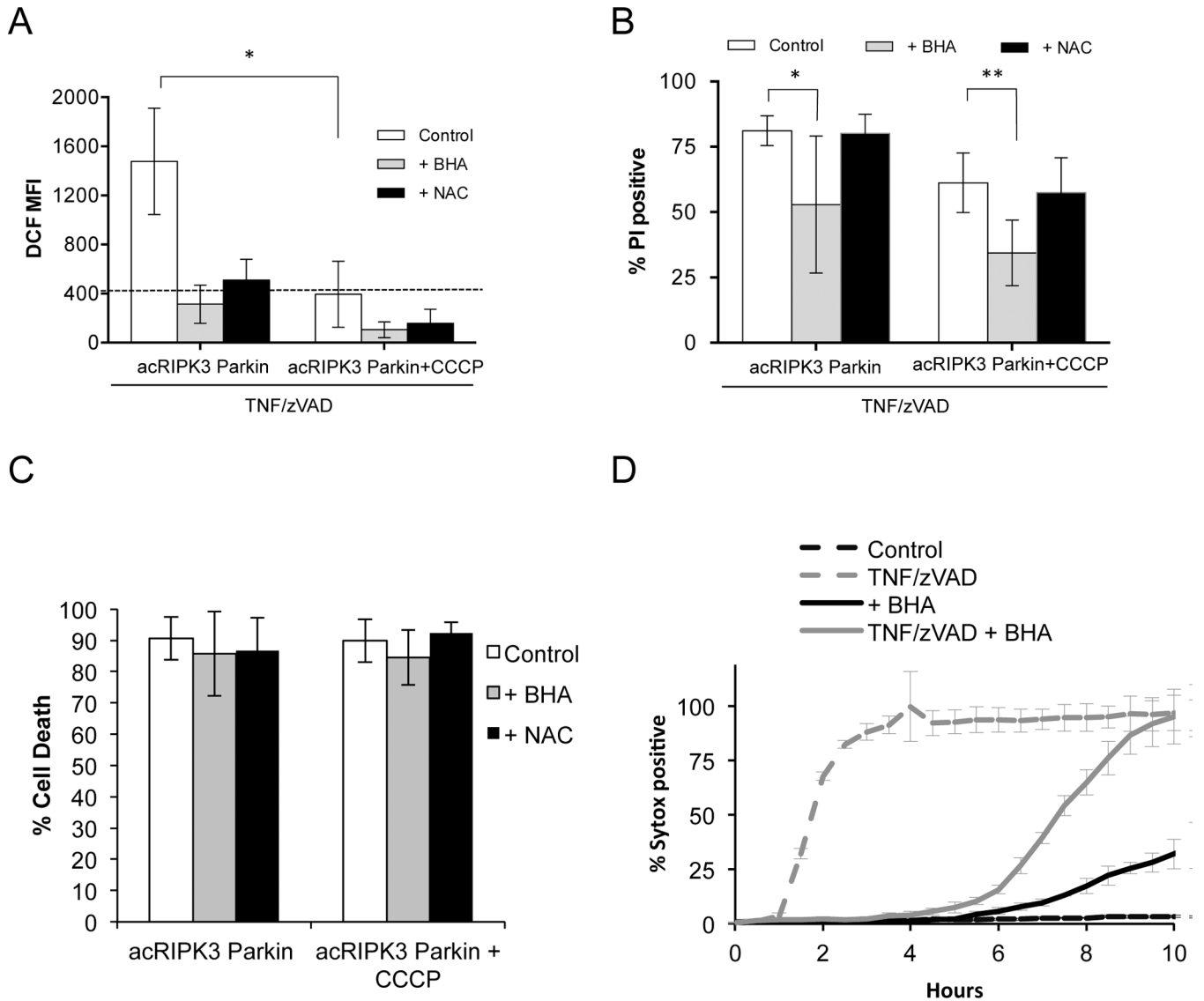
Figure 4. Elimination of mitochondria prevents necroptosis-associated ROS production, but does not alter RIPK3-dependent cell death

A. NIH-3T3 cells expressing acRIPK3 and Parkin were treated with CCCP to induce mitochondrial elimination, then treated with TNF+zVAD for 2 hours in the presence of the ROS scavangers butyrated hydroxyanisole (BHA) or N-acetylcysteine (NAC). ROS production was measured using the dye DCF. MFI=Mean Fluorescent Intensity. Results shown are the mean ± S.D. of n 3 independent experiments. *, P<0.001. Black dotted line corresponds to the basal level of ROS in the Control at t=0. **B.** NIH-3T3 cells treated like in **A** for 4 hours, were stained with PI and cell death was determined by flow cytometry (mean ± S.D. of n 3 independent experiments). *, P<0.05, **, P=0.0518 (*t* test). **C.** Mitochondria were depleted as in **A,** and RIPK3 dimerization was triggered in the presence of BHA or NAC. 2 hours later cell death was quantified as in **B**. (mean ± S.D. of n 3 independent experiments) **D.** Mitochondria depletion was triggered in NIH-3T3 cells as in **A**, and cells were then treated with TNF+zVAD and BHA as indicated. Cell death was measured by Sytox Green uptake over time in an IncuCyte imager. Data show one representative experiment of three independent experiments. See also Figure S3.